Geophys. J. Int. (1999) **136,** 341–356

The tensile dislocation problem in a layered elastic medium

Maurizio Bonafede and Eleonora Rivalta

Dipartimento di Fisica, Universita di Bologna, Settore di Geofisica, Viale Berti-Pichat 8, *Bologna* 40127, *Italy. E-mail: bonafede@ibogfs.df.unibo.it*

Accepted 1998 August 11. Received 1998 July 2; in original form 1998 April 23

SUMMARY

Tensile dislocations are often employed to model magma intrusion within volcanic edifices through lateral or feeding dykes. In spite of the large heterogeneity inferred (e.g. from seismic tomography studies) in volcanic areas, most crack models of dykes so far have been developed in homogeneous media. In this paper the simplest elastic medium is considered, consisting of two welded half-spaces, characterized by different elastic parameters. A plane-strain configuration is assumed. The elementary dislocation problem is solved in which a constant Burgers vector is assigned along a rectilinear dislocation line parallel to the plane separating the two half-spaces; the dislocation surface is a half-plane orthogonal to the interface and bounded by the dislocation line. Case I is considered first, in which the dislocation surface is entirely contained in one half-space (half-space 1). Explicit analytic solutions are provided for all components of the displacement and stress fields all over the medium; these are found to reproduce previously published results, which were, however, limited to the dislocation plane and to one component of stress. If the rigidity of the half-space 2 vanishes, the present results reproduce the solutions for the tensile dislocation problem in a half-space with a free surface. Explicit solutions are furthermore given for case II, in which the dislocation line is in the half-space 2 and the dislocation surface cuts the interface between the two media and all of the half-space 1. Finally, closed dislocation surfaces, bounded in the dip direction, are obtained by the superposition of solutions pertinent to two different dislocation lines, and stress fields are compared with solutions in a homogeneous unbounded medium endowed with the same elastic parameters assumed for the harder half-space 1. Results for all non-vanishing stress components are shown graphically in two models: in model A both dislocation lines are embedded in half-space 1; in model B, one dislocation line is embedded in half-space 1 and the other in half-space 2. Stress components, which must be continuous across the interface between the hard and soft half-spaces, are found to be significantly lower in the harder half-space than in the homogeneous model. On the other hand, the stress component normal to the dislocation surface, which is not involved in the welded boundary condition, is significantly higher along the hard side of the interface in model A, while in model B it is significantly lower near the dislocation–interface crossing. The importance of analytical solutions for the elementary dislocation problem in a layered medium is strengthened by their role as integral kernels to be employed in crack models of pressurized dykes.

Key words: dyke emplacement, layered media, tensile dislocations.

INTRODUCTION

Dykes intruding the crust modify the pre-existing stress in the crust, giving rise to the ground deformation episodes and seismic events which are commonly observed in volcanic areas. Great attention has been devoted up to now to modelling the surface displacement produced by dykes in terms of dislocation sources with a constant Burgers vector opening in a homogeneous

half-space (e.g. Davis 1983; Okada 1992) or as cracks with an assigned overpressure (e.g. Pollard & Holzhausen 1979; Dieterich & Decker 1975; Pollard *et al.* 1983). More recently, the influence of the topographic load provided by the volcanic edifice has been also accounted for (Cayol 1996). Apart from academic aspects, the interest in finding a realistic solution of the dyke deformation problem lies in the possibility of extracting, from geodetic and seismic data, information on the position, depth, magma content and geometry of a buried dyke, with obvious implications for civil protection purposes should an eruption ensue (Zlotnicki *et al.* 1990; Bonaccorso & Davis 1993; Murray 1994). The stress induced by dyke opening is also thought to be responsible for the seismicity generally observed prior to an eruption (e.g. Lénat *et al.* 1989a,b; Ferrucci & Patanè 1993; Cocina *et al.* 1996a), for inducing isotropic moment tensor components (e.g. Dahm & Brandsdottir 1997), and even for causing sharp changes in the principal stress directions (e.g. Cocina *et al.* 1996b).

However, most models developed so far have paid little attention to the stress field induced by dyke injection, and even less attention has been devoted to studying the effects of the structural heterogeneities present in volcanic regions. Geophysical prospecting and seismic tomography show that this is an oversimplification of reality, since high-rigidity layers are generally present at depth below a volcanic edifice, covered by much softer volcano-sedimentary layers composed of a complex mixture of ash, mud, lava flows and pyroclastic material. Dahm (1996) recently provided numerical solutions for dislocation sources in multilayered media, employing a boundary element technique (e.g. Crouch & Starfield 1990). This technique splits the fracture surface into a finite number of elementary dislocation sources, each embedded in a homogeneous layer, and the discontinuities appearing over layer interfaces are removed using fictitious dislocation sources. Other attempts to model dislocation sources in heterogeneous media are restricted to point sources (e.g. Rundle 1980; Roth 1990; Fernandez & Rundle 1994).

Furthermore, magma uprise from the mantle is generally described in terms of positive buoyancy, related to the magma density being lower than that of the host rock, up to a neutral buoyancy level where the density contrast reverses its sign (e.g. Lister 1991). Since major density changes are generally accompanied by rigidity changes, for example along structural discontinuities such as the Moho, stress changes occurring when a dyke comes close to a structural discontinuity cannot be ignored when studying the arrest of dyke propagation. Indeed, buried dykes are often seen to become arrested against structural discontinuities.

In this paper analytic solutions in closed form are derived for the displacement and stress fields produced by a vertical tensile dislocation with constant opening (Burgers vector) in the proximity of the boundary surface between two media characterized by different elastic parameters. Over the boundary surface, displacement and traction components are made continuous (welded boundary conditions). Solutions will be provided for the case in which the dislocation surface is entirely embedded in one half-space (case I) and the case in which the dislocation surface cuts across the interace between the two half-spaces (case II).

It is noted that case I was considered by Cook (1971) (see also Erdogan *et al.* 1973), whose analysis was, however, limited to only one component of the stress field and restricted to the plane containing the dislocation surface. In the following, a different technique of solution is employed, Cook's results are reproduced, and solutions are provided for all displacement and stress components all over the two half-spaces. If the rigidity of one of the two half-spaces vanishes, case I furthermore reproduces the solutions for an elementary dislocation in a half-space bounded by a free surface (e.g Bonafede & Danesi 1997).

This model is thought to provide useful insights into stress changes induced by a magma-filled dyke buried at depth in a volcanic region characterized by strong vertical heterogeneities. Further important complications which would be introduced by the presence of a free surface, for example, are for the moment ignored. Accordingly, the application of the present results to real cases of dyke injection must be restricted to buried dykes far below the ground surface. These solutions moreover provide the integral kernels required for computing displacement and stress fields in the crack problem, which will be the subject of another paper. In the next section the technique of solution is described in some detail; explicit solutions for both case I and case II are provided in the following sections; finally results are plotted and discussed in the last section.

THE ELEMENTARY DISLOCATION PROBLEM

Let us consider an elementary tensile dislocation embedded in a layered elastic medium composed of two welded half-spaces endowed with different elastic properties (Fig. 1). The discontinuity in the displacement field gives rise to displacement and stress fields in the surrounding medium which will be computed starting from the mode I singular solution for an unbounded homogeneous medium. Such a solution for the displacement field does not depend on rigidity but depends explicitly on the Poisson ratio (see below); from the displacement components stress fields can be computed employing Hooke's law separately for each half-space. Of course, displacements and tractions computed in this way would be discontinuous over the interface. These discontinuities will be removed by computing the effects that they cause on each half-space and subtracting these solutions from the homogeneous dislocation fields. To this end, the Galerkin method will be employed (e.g. Fung 1965) to compute stress and displacement components produced in a half-space $z > 0$ (or $z < 0$) by the application of assigned loads distributed over the surface $z = 0$. Applications of the Galerkin method to dislocation problems in a half-space with a free surface can be found in Maruyama (1964).

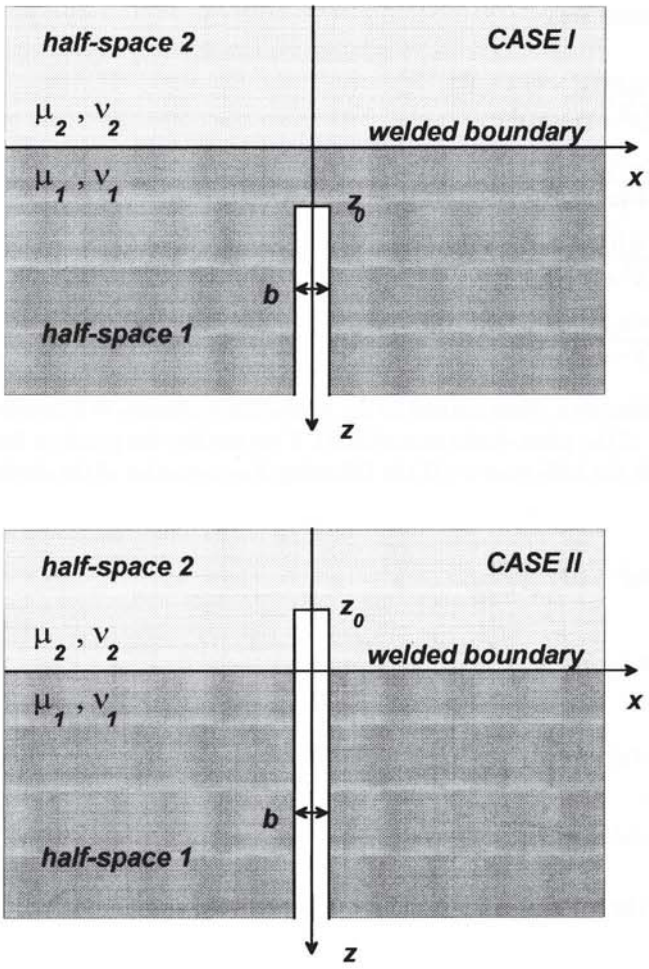

Figure 1. Sketch of the elementary dislocation problem in the layered medium. The lower half-space in $z>0$ has a Poisson ratio ν_1 and a rigidity μ_1; it is welded to the 'upper' half-space (Poisson ratio ν_2 and rigidity μ_2) along the plane $z=0$. A tensile dislocation line is present in $x=0$, $z=z_0$; the dislocation surface goes from $z=z_0$ to $z=\infty$. The face $x=0^+$ of the dislocation surface is displaced in the x-direction by $b/2$, the face $x=0^-$ is displaced by the same amount in the opposite direction. Case I: the dislocation line is in the half-space $z_0>0$. Case II: the dislocation line is in the half-space $z_0<0$.

Discontinuities over the interface

Let us consider a tensile elementary dislocation in an unbounded homogeneous medium characterized by rigidity μ and Poisson ratio ν. We shall assume a plane-strain configuration; the dislocation is defined through a constant Burgers vector $\mathbf{b}=b\hat{\mathbf{i}}$ and dislocation line $x=0$, $z=z_0$ parallel to the y-axis (e.g. Landau & Lifschitz 1967, pp. 156–185). Apart from an arbitrary translation, the displacement components generated by this elementary dislocation in an unbounded medium can be written as (e.g. Bonafede & Danesi 1997)

$$\begin{cases} u_x^{(\infty)}(x,z,z_0)=\dfrac{b}{2\pi}\left[\operatorname{Arctan}\dfrac{z-z_0}{x}+\dfrac{1}{2(1-\nu)}\dfrac{x(z-z_0)}{x^2+(z-z_0)^2}\right] \\ u_z^{(\infty)}(x,z,z_0)=-\dfrac{b}{4\pi(1-\nu)}\left[(1-2\nu)\ln\sqrt{\dfrac{x^2+(z-z_0)^2}{z_0^2}}-\dfrac{(z-z_0)^2}{x^2+(z-z_0)^2}\right] \end{cases}, \tag{1}$$

where the superscript (∞) indicates that this is the solution for a homogeneous unbounded medium and

$$\operatorname{Arctan}\frac{z-z_0}{x}=\begin{cases}\dfrac{\pi}{2}+\arctan\dfrac{z-z_0}{x} & \text{if } x>0 \\ -\dfrac{\pi}{2}+\arctan\dfrac{z-z_0}{x} & \text{if } x<0\end{cases}.$$

Non-vanishing stress components are

$$\begin{cases} \sigma_{xx}^{(\infty)}(x, z, z_0) = -\dfrac{b\mu}{2\pi(1-\nu)} \dfrac{(z-z_0)[3x^2+(z-z_0)^2]}{[x^2+(z-z_0)^2]^2} \\ \sigma_{xz}^{(\infty)}(x, z, z_0) = -\dfrac{b\mu}{2\pi(1-\nu)} \dfrac{x[(z-z_0)^2-x^2]}{[x^2+(z-z_0)^2]^2} \\ \sigma_{zz}^{(\infty)}(x, z, z_0) = -\dfrac{b\mu}{2\pi(1-\nu)} \dfrac{(z-z_0)[(z-z_0)^2-x^2]}{[x^2+(z-z_0)^2]^2} \\ \sigma_{yy}^{(\infty)}(x, z, z_0) = -\dfrac{b\mu\nu}{\pi(1-\nu)} \dfrac{(z-z_0)}{x^2+(z-z_0)^2} \end{cases} . \tag{2}$$

For the choice of the welded interface as a plane normal to the z-axis, the continuity of tractions implies continuity of σ_{xz} and σ_{zz} (σ_{yz} vanishing identically because of the plane-strain assumption). If we employ the previous formulae, substituting μ_1, ν_1 for μ, ν in the half-space $z>0$ and μ_2, ν_2 in the half-space $z<0$, the following discontinuities of the displacement and traction components would appear in $z=0$:

$$\begin{cases} \Delta u_x(x, z_0) = u_{x2}^{(\infty)}(x, z_0) - u_{x1}^{(\infty)}(x, z_0) = -b\gamma \dfrac{xz_0}{x^2+z_0^2} \\ \Delta u_z(x, z_0) = u_{z2}^{(\infty)}(x, z_0) - u_{z1}^{(\infty)}(x, z_0) = b\gamma \left[\ln \sqrt{\dfrac{x^2+z_0^2}{z_0^2}} + \dfrac{z_0^2}{x^2+z_0^2} \right] \end{cases} , \tag{3}$$

$$\begin{cases} \Delta\sigma_{xz}(x, z_0) = \sigma_{xz2}^{(\infty)}(x, z_0) - \sigma_{xz1}^{(\infty)}(x, z_0) = b\delta \dfrac{x[x^2-z_0^2]}{[x^2+z_0^2]^2} \\ \Delta\sigma_{zz}(x, z_0) = \sigma_{zz2}^{(\infty)}(x, z_0) - \sigma_{zz1}^{(\infty)}(x, z_0) = -b\delta \dfrac{z_0[x^2-z_0^2]}{[x^2+z_0^2]^2} \end{cases} , \tag{4}$$

where subscripts 1 and 2 refer to the half-spaces $z>0$ and $z<0$, respectively, and

$$\gamma = \frac{1}{4\pi}\left[\frac{1}{(1-\nu_2)} - \frac{1}{(1-\nu_1)}\right],$$

$$\delta = \frac{1}{2\pi}\left[\frac{\mu_2}{(1-\nu_2)} - \frac{\mu_1}{(1-\nu_1)}\right]. \tag{5}$$

In the following it is convenient to deal with square-integrable functions; accordingly, instead of imposing the continuity of displacement components over $z=0$, we shall impose the continuity of their x-derivatives. The two conditions are equivalent, since no dependence on y is allowed by the plane-strain assumption, and displacements are defined in the theory of elasticity within an arbitrary additive constant (which can be appropriately chosen *a posteriori*).

Fourier components of discontinuities (case I)

In the following it is necessary to distinguish between the two possibilities $z_0>0$ (case I) and $z_0<0$ (case II).

As will be shown in the next section, the discontinuities over the plane $z=0$ can easily be accounted for if they are harmonic functions of x. To this end, the harmonic components of (4) and of the x-derivatives of (3) are given below for case I ($z_0>0$):

$$\begin{cases} \Delta\sigma_{zz}(x, z_0) = b\delta \dfrac{z_0[z_0^2-x^2]}{[z_0^2+x^2]^2} = b\delta \displaystyle\int_0^{+\infty} \xi(k)\cos kx\, dk \\ \Delta\sigma_{xz}(x, z_0) = -b\delta \dfrac{x[z_0^2-x^2]}{[z_0^2+x^2]^2} = b\delta \displaystyle\int_0^{+\infty} \zeta(k)\sin kx\, dk \\ \Delta\dfrac{\partial u_x}{\partial x}(x, z_0) = -b\gamma \dfrac{z_0[z_0^2-x^2]}{[z_0^2+x^2]^2} = -b\gamma \displaystyle\int_0^{+\infty} \xi(k)\cos kx\, dk \\ \Delta\dfrac{\partial u_z}{\partial x}(x, z_0) = -b\gamma \dfrac{x[z_0^2-x^2]}{[z_0^2+x^2]^2} = b\gamma \displaystyle\int_0^{+\infty} \zeta(k)\sin kx\, dk \end{cases} , \tag{6}$$

where δ and γ are defined in (5) and the Fourier transforms $\xi(k)$ and $\zeta(k)$ are easily computed employing the theorem of residues (in employing it, the integration path must be chosen appropriately according to whether z_0 and k are positive or negative). In the present section we shall assume $z_0 > 0$ for definiteness. In the following section results will be shown for case II. In case I we find

$$\begin{cases} \xi(k) = kz_0 \, e^{-kz_0} \\ \zeta(k) = (1 - kz_0) \, e^{-kz_0} \end{cases} \qquad z_0 > 0 . \tag{7}$$

Employing the superposition principle we can now address the subproblem of computing the displacement and stress fields in the half-spaces $z > 0$ and $z < 0$ generated by harmonic discontinuities over the boundary $z = 0$.

The Galerkin method (case I)

The Galerkin method can be profitably employed to obtain elastostatic solutions in a half-space when tractions or displacements are assigned over its surface (e.g. Fung 1965). These solutions are particularly simple if the boundary conditions are harmonically modulated over the surface $z = 0$. This is not restrictive since any square-integrable function can generally be expanded in this way through Fourier transforms. Let us denote by subscripts 1 and 2 boundary conditions to be imposed on the half-spaces 1 ($z > 0$) and 2 ($z < 0$), respectively. The discontinuities (6) to be removed are either odd or even functions of x; symmetry considerations and the plane-strain assumption allow a restriction to the following expressions for the boundary conditions:

$$\begin{cases} \sigma_{zz1}(x, z = 0) = A_1(k) \cos kx \\ \sigma_{xz1}(x, z = 0) = B_1(k) \sin kx \\ \sigma_{yz1}(x, z = 0) = 0 \\ \sigma_{ij1}(z \to +\infty) = 0 \qquad \forall i, j \end{cases} , \qquad \begin{cases} \sigma_{zz2}(x, z = 0) = A_2(k) \cos kx \\ \sigma_{xz2}(x, z = 0) = B_2(k) \sin kx \\ \sigma_{yz2}(x, z = 0) = 0 \\ \sigma_{ij2}(z \to -\infty) = 0 \qquad \forall i, j \end{cases} , \tag{8}$$

where $A_1(k), \ldots, B_2(k)$ are functions of the wavenumber k to be determined.

Solutions in the two half-spaces can be obtained employing two Galerkin vectors (one for each half-space) with one non-vanishing component $\mathbf{G}_1 = (0, 0, Z_1)$, $\mathbf{G}_2 = (0, 0, Z_2)$, where Z_1 and Z_2 must be biharmonic functions in order to satisfy the equations of equilibrium. Z_1 and Z_2 are also termed Love's strain functions. We denote Z_1 and Z_2 by Z when it is not necessary to distinguish between them. Once a strain function Z is known, displacement components related to it can be found from

$$u_i^G = \frac{1 - \nu}{\mu} G_{i,jj} - \frac{1}{2\mu} G_{j,ji} ,$$

where two repeated subscripts denote contraction and subscripts preceded by a comma are employed to denote partial derivatives (e.g. $G_{i,jj} = \nabla^2 G_i$). Stress components can be obtained from the previous formulae employing Hooke's law.

Under very general assumptions, a biharmonic function Z can be written as (e.g. Fung 1965, p. 206)

$$Z(x, z) = (\alpha + \beta kz)\psi(x, z) , \tag{9}$$

where ψ is a harmonic function and α, β are constants to be determined. The boundary conditions suggest the following choice for ψ:

$$\psi(x, z) = \cos kx f(z) , \qquad f(z) = a \, e^{-kz} + b \, e^{+kz} , \tag{10}$$

where the expression for $f(z)$ is imposed by $\nabla^2 \psi = 0$. After imposing the boundary conditions (8) at infinity, only one exponential term is retained in each half-space and the multiplicative constants a, b become inessential:

$$\begin{cases} Z_1 = (\alpha_1 + \beta_1 kz) \, e^{-kz} \cos kx & \text{in } z > 0 \\ Z_2 = (\alpha_2 + \beta_2 kz) \, e^{+kz} \cos kx & \text{in } z < 0 \end{cases} . \tag{11}$$

From the relations between the strain function Z and the displacement and stress fields, the following results are obtained:

$$\begin{cases} u_{x1}^G = \dfrac{k^2}{2\mu_1} (-\alpha_1 + \beta_1 - \beta_1 kz) \, e^{-kz} \sin kx \\ u_{x2}^G = \dfrac{k^2}{2\mu_2} (\alpha_2 + \beta_2 + \beta_2 kz) \, e^{kz} \sin kx \\ u_{z1}^G = \dfrac{k^2}{2\mu_1} [-\alpha_1 - 2\beta_1 (1 - 2\nu_1) - \beta_1 kz] \, e^{-kz} \cos kx \\ u_{z2}^G = \dfrac{k^2}{2\mu_2} [-\alpha_2 + 2\beta_2 (1 - 2\nu_2) - \beta_2 kz] \, e^{kz} \cos kx \end{cases} , \tag{12}$$

$$\begin{cases} \sigma^G_{xz1} = (\alpha_1 - 2\beta_1\nu_1 + \beta_1 kz)k^3\,\mathrm{e}^{-kz}\sin kx \\ \sigma^G_{xz2} = (\alpha_2 + 2\beta_2\nu_2 + \beta_2 kz)k^3\,\mathrm{e}^{kz}\sin kx \\ \sigma^G_{zz1} = [\alpha_1 + \beta_1(1-2\nu_1) + \beta_1 kz]k^3\,\mathrm{e}^{-kz}\cos kx \\ \sigma^G_{zz2} = [-\alpha_2 + \beta_2(1-2\nu_2) - \beta_2 kz]k^3\,\mathrm{e}^{kz}\cos kx \\ \sigma^G_{xx1} = [-\alpha_1 + \beta_1(1+2\nu_1) - \beta_1 kz]k^3\,\mathrm{e}^{-kz}\cos kx \\ \sigma^G_{xx2} = [\alpha_2 + \beta_2(1+2\nu_2) + \beta_2 kz]k^3\,\mathrm{e}^{kz}\cos kx \\ \sigma^G_{yy1} = 2\nu_1\beta_1 k^3\,\mathrm{e}^{-kz}\cos kx \\ \sigma^G_{yy2} = 2\nu_2\beta_2 k^3\,\mathrm{e}^{kz}\cos kx \end{cases} \tag{13}$$

If we now impose the remaining boundary conditions (8), four linear equations are obtained for α_1, α_2, β_1, β_2 in terms of $A_1(k)$, $A_2(k)$, $B_1(k)$, $B_2(k)$:

$$\begin{cases} \alpha_1 = \dfrac{2\nu_1 A_1 + (1-2\nu_1)B_1}{k^3} \\ \alpha_2 = \dfrac{-2\nu_2 A_2 + (1-2\nu_2)B_2}{k^3} \\ \beta_1 = \dfrac{A_1 - B_1}{k^3} \\ \beta_2 = \dfrac{A_2 + B_2}{k^3} \end{cases} \tag{14}$$

Finally, we can evaluate the x-derivatives of the displacement field generated in both half-spaces by the loads (8):

$$\begin{cases} \dfrac{\partial u^G_{x1}}{\partial x} = \dfrac{\mathrm{e}^{-kz}\cos kx}{2\mu_1}[(1-2\nu_1)A_1(k) - 2(1-\nu_1)B_1(k) - [A_1(k) - B_1(k)]kz] \\ \dfrac{\partial u^G_{x2}}{\partial x} = \dfrac{\mathrm{e}^{kz}\cos kx}{2\mu_2}[(1-2\nu_2)A_2(k) + 2(1-\nu_2)B_2(k) + [A_2(k) + B_2(k)]kz] \\ \dfrac{\partial u^G_{z1}}{\partial x} = -\dfrac{\mathrm{e}^{-kz}\sin kx}{2\mu_1}[-2(1-\nu_1)A_1(k) + (1-2\nu_1)B_1(k) - [A_1(k) - B_1(k)]kz] \\ \dfrac{\partial u^G_{z2}}{\partial x} = -\dfrac{\mathrm{e}^{kz}\sin kx}{2\mu_2}[2(1-\nu_2)A_2(k) + (1-2\nu_2)B_2(k) - [A_2(k) + B_2(k)]kz] \end{cases} \tag{15}$$

The stress components generated by the same loads are

$$\begin{cases} \sigma^G_{zz1}(x,z;k) = [(A_1(k) + (A_1(k) - B_1(k))kz]\,\mathrm{e}^{-kz}\cos kx \\ \sigma^G_{zz2}(x,z;k) = [(A_2(k) - (A_2(k) + B_2(k))kz]\,\mathrm{e}^{kz}\cos kx \\ \sigma^G_{xz1}(x,z;k) = [(B_1(k) + (A_1(k) - B_1(k))kz]\,\mathrm{e}^{-kz}\sin kx \\ \sigma^G_{xz2}(x,z;k) = [(B_2(k) + (A_2(k) + B_2(k))kz]\,\mathrm{e}^{kz}\sin kx \\ \sigma^G_{xx1}(x,z;k) = [(A_1(k) - 2B_1(k) - (A_1(k) - B_1(k))kz]\,\mathrm{e}^{kz}\cos kx \\ \sigma^G_{xx2}(x,z;k) = [(A_2(k) + 2B_2(k) + (A_2(k) + B_2(k))kz]\,\mathrm{e}^{-kz}\cos kx \\ \sigma^G_{yy1}(x,z;k) = 2\nu_1(A_1(k) - B_1(k))\,\mathrm{e}^{-kz}\cos kx \\ \sigma^G_{yy2}(x,z;k) = 2\nu_2(A_2(k) + B_2(k))\,\mathrm{e}^{kz}\cos kx \end{cases} \tag{16}$$

In our dislocation problem, we are interested in removing the jump discontinuities (6) of displacements and tractions over the plane $z = 0$. We can now arrange a linear system to determine the coefficients A_1, A_2, B_1, B_2 [defining the strain functions Z_1 and Z_2 through (11) and (14)] which are required to remove the harmonic components of the discontinuities (6).

Matching the discontinuities (case I)

The linear system mentioned above is

$$\mathbf{M}\begin{pmatrix} A_2 \\ A_1 \\ B_2 \\ B_1 \end{pmatrix} = b\begin{pmatrix} \delta\xi(k) \\ \delta\zeta(k) \\ -\gamma\xi(k) \\ \gamma\zeta(k) \end{pmatrix}, \tag{17}$$

where $\xi(k)$ and $\zeta(k)$ are given by (7) and the matrix $\mathbf{M}$ is

$$\mathbf{M} = \begin{pmatrix} 1 & -1 & 0 & 0 \\ 0 & 0 & 1 & -1 \\ \dfrac{1-2\nu_2}{2\mu_2} & -\dfrac{1-2\nu_1}{2\mu_1} & \dfrac{1-\nu_2}{\mu_2} & \dfrac{1-\nu_1}{\mu_1} \\ -\dfrac{1-\nu_2}{\mu_2} & -\dfrac{1-\nu_1}{\mu_1} & -\dfrac{1-2\nu_2}{2\mu_2} & \dfrac{1-2\nu_1}{2\mu_1} \end{pmatrix}. \tag{18}$$

Hence

$$(A_2, A_1, B_2, B_1)^{\mathrm{T}} = b\mathbf{M}^{-1}(\delta\xi(k), \delta\zeta(k), -\gamma\xi(k), \gamma\zeta(k))^{\mathrm{T}}. \tag{19}$$

The inverse matrix $\mathbf{M}^{-1}$ can be written as

$$\mathbf{M}^{-1} = \frac{1}{(e-d)(e+d)}\begin{pmatrix} a_1+c^+ & c^- & -d & -e \\ -(a_2+c^+) & c^- & -d & -e \\ c^- & a_1+c^+ & e & d \\ c^- & -(a_2+c^+) & e & d \end{pmatrix}, \tag{20a}$$

where

$$\begin{aligned} a_1 &= \frac{3-4\nu_1}{4\mu_1^2}, & a_2 &= \frac{3-4\nu_2}{4\mu_2^2}, \\ c^- &= \frac{1-(3-4\nu_1)(3-4\nu_2)}{8\mu_1\mu_2}, & c^+ &= \frac{1+(3-4\nu_1)(3-4\nu_2)}{8\mu_1\mu_2}, \\ d &= \frac{1-2\nu_2}{2\mu_2} - \frac{1-2\nu_1}{2\mu_1}, & e &= \frac{1-\nu_2}{\mu_2} + \frac{1-\nu_1}{\mu_1}. \end{aligned} \tag{20b}$$

From (19) we can compute analytically the coefficients $A_1(k)$, $A_2(k)$, $B_1(k)$, $B_2(k)$ as functions of the wavenumber k. These will be inserted into (15) and (16) and the resulting solutions will be integrated in dk to obtain the stress fields generated by the discontinuities (6). The solution of the original problem (i.e. the elastostatic solution in a medium formed by two welded half-spaces) is finally obtained by subtracting from the unbounded space solution (eqs 1–2) (responsible for the appearance of discontinuities) the strain function contributions for the half-spaces $z<0$ and $z>0$ (which were built in such a way as to reproduce the same discontinuities over the interface $z=0$).

The integrals I_{ij} involved in synthesizing the response of the two half-spaces to the discontinuities (6)–(7) are of the type

$$\int_0^{+\infty} \mathrm{e}^{-k(\pm z+z_0)}\begin{Bmatrix}\cos kx \\ \sin kx\end{Bmatrix} k^n\,dk, \qquad n=0,1,2. \tag{21}$$

These can easily be computed analytically and are given by eq. (A1).

Employing the definitions of I_{ij} given in the Appendix, the solution can be written most simply by defining a row matrix $\boldsymbol{\sigma}^G$

$$\boldsymbol{\sigma}^G = (\sigma^G_{zz1} \quad \sigma^G_{zz2} \quad \sigma^G_{xz1} \quad \sigma^G_{xz2}).$$

The following expression is obtained:

$$\sigma_i^G = b\sum_{j=1}^{4} G^{\mathrm{I}}_{ij} I_{ij} \qquad \text{(no sum over } i\text{)}, \tag{22}$$

where superscript I denotes case I and

$$\mathbf{G}^{\mathrm{I}}=\begin{pmatrix} D & -(C_2-D) & C_2-D & 2(C_2-D) \\ D & -(C_1+D) & C_1-D & 0 \\ C_2 & -(C_2-D) & -(C_2-D) & 2(C_2-D) \\ C_1 & (C_1+D) & -(C_1-D) & 0 \end{pmatrix}, \tag{23}$$

with

$$\begin{aligned} C_1&=\frac{1}{(e^2-d^2)}[\delta(a_1+c^+)+\gamma d], \\ C_2&=\frac{1}{(e^2-d^2)}[-\delta(a_2+c^+)+\gamma d], \\ D&=\frac{1}{(e^2-d^2)}[\delta c^- -\gamma e], \end{aligned} \tag{24}$$

a_1, a_2, c^-, c^+, d, e being defined in (20b) and δ, γ in (5).

Other stress components (which need not be continuous on $z=0$) are given by

$$\begin{cases} \dfrac{1}{b}\sigma^G_{xx1}=-(2C_2-D)I_{11}+(C_2-D)I_{12}+3(C_2-D)I_{13}-2(C_2-D)I_{14} \\ \dfrac{1}{b}\sigma^G_{xx2}=(2C_1+D)I_{21}+(C_1+D)I_{22}-(C_1-D)I_{23} \\ \dfrac{1}{b}\sigma^G_{yy1}=2\nu_1(C_2-D)(2I_{13}-I_{11}) \\ \dfrac{1}{b}\sigma^G_{yy2}=2\nu_2(C_1+D)I_{21} \end{cases} \tag{25}$$

Analytic expressions for the displacement components are finally obtained by integrating (15) in dk and then in dx; this requires computing the primitives of I_{ij} with respect to x, which are given by eq. (A2):

$$Y_{ij}(x,z;z_0)=\int I_{ij}(x,z;z_0)\,dx. \tag{26}$$

Accordingly, contributions to the displacement components for case I due to the strain function

$$\begin{cases} u^G_{x1}(x,z;z_0)=b\sum_{j=1}^{4} U^{\mathrm{I}}_{1j}Y_{1j}(x,z;z_0) \\ u^G_{x2}(x,z;z_0)=b\sum_{j=1}^{4} U^{\mathrm{I}}_{2j}Y_{2j}(x,z;z_0) \end{cases}, \quad \begin{cases} u^G_{z1}(x,z;z_0)=b\sum_{j=1}^{4} U^{\mathrm{I}}_{3j}Y_{3j}(x,z;z_0) \\ u^G_{z2}(x,z;z_0)=b\sum_{j=1}^{4} U^{\mathrm{I}}_{4j}Y_{4j}(x,z;z_0) \end{cases}, \tag{27}$$

where $\mathbf{U}^{\mathrm{I}}$ is the following matrix

$$\mathbf{U}^{\mathrm{I}}=\begin{pmatrix} -\dfrac{(1-\nu_1)}{\mu_1}C_2+\dfrac{(1-2\nu_1)}{2\mu_1}D & \dfrac{1}{2\mu_1}(C_2-D) & \dfrac{(3-4\nu_1)}{2\mu_1}(C_2-D) & -\dfrac{1}{\mu_1}(C_2-D) \\ \dfrac{(1-\nu_2)}{\mu_2}C_1+\dfrac{(1-2\nu_2)}{2\mu_2}D & \dfrac{1}{2\mu_2}(C_1+D) & -\dfrac{1}{2\mu_2}(C_1-D) & 0 \\ \dfrac{(1-\nu_1)}{\mu_1}D-\dfrac{(1-2\nu_1)}{2\mu_1}C_2 & -\dfrac{1}{2\mu_1}(C_2-D) & \dfrac{(3-4\nu_1)}{2\mu_1}(C_2-D) & \dfrac{1}{\mu_1}(C_2-D) \\ -\dfrac{(1-\nu_2)}{\mu_2}D-\dfrac{(1-2\nu_2)}{2\mu_2}C_1 & \dfrac{1}{2\mu_2}(C_1+D) & -\dfrac{1}{2\mu_2}(C_1-D) & 0 \end{pmatrix} \tag{28}$$

and C_1, C_2, D are given in (24).

The elementary dislocation solutions $u_{i1}^{(el)}$, $u_{i2}^{(el)}$ and $\sigma_{ij1}^{(el)}$, $\sigma_{ij2}^{(el)}$ in a medium formed by two welded half-spaces is obtained after subtracting the displacement u_i^G and stress σ_{ij}^G fields from the unbounded-space solutions $u_i^{(\infty)}$ and $\sigma_{ij}^{(\infty)}$ (eqs 1–2):

$$u_{i1-2}^{(el)} = u_{i1-2}^{(\infty)} - u_{i1-2}^{G}, \qquad \sigma_{ij1-2}^{(el)} = \sigma_{ij1-2}^{(\infty)} - \sigma_{ij1-2}^{G}. \tag{29}$$

Note that in solving the elementary dislocation problem, we imposed the continuity of x-derivatives of the displacement. The displacement obtained according to the previous scheme might then contain terms discontinuous across the interface $z=0$. Checking previous formulae, it is seen that no such discontinuity is present (in fact this was the reason for choosing, among the infinite primitives of I_{ij}, the determinations Y_{ij} given by eq. (A2).

EXPLICIT SOLUTIONS FOR CASES I AND II

In order to complete the solution derived under the assumption that $z_0 > 0$ (case I), we must also solve the problem when the dislocation line is in the half-space $z<0$ (case II), i.e. a dislocation surface given by the half-plane $x=0$, $z>z_0$ with $z_0<0$. Eqs (1)–(6) are valid without change if $z_0<0$; however, the Fourier transforms in (7) need to be computed again when $z_0<0$. Without duplicating the previous procedure, we write in the following the final solutions u_i and σ_{ij} for both cases [the superscript (el) employed in (29) to denote the elementary dislocation solution will now be dropped].

Case I

The displacement field generated by an elementary dislocation opening in a layered medium when $z_0>0$ is

$$\begin{cases}
\dfrac{1}{b}u_{x1}(x,z,z_0) = \dfrac{1}{2\pi}\left[-\operatorname{Arctan}\dfrac{z-z_0}{x} + \dfrac{1}{2(1-\nu_1)}\dfrac{x(z-z_0)}{x^2+(z-z_0)^2}\right] - \displaystyle\sum_{j=1}^{4} U^{\mathrm{I}}_{1j}Y_{1j} \\
\dfrac{1}{b}u_{x2}(x,z,z_0) = \dfrac{1}{2\pi}\left[-\operatorname{Arctan}\dfrac{z-z_0}{x} + \dfrac{1}{2(1-\nu_2)}\dfrac{x(z-z_0)}{x^2+(z-z_0)^2}\right] - \displaystyle\sum_{j=1}^{4} U^{\mathrm{I}}_{2j}Y_{2j} \\
\dfrac{1}{b}u_{z1}(x,z,z_0) = -\dfrac{1}{4\pi(1-\nu_1)}\left[(1-2\nu_1)\ln\sqrt{\dfrac{x^2+(z-z_0)^2}{z_0^2}} - \dfrac{(z-z_0)^2}{x^2+(z-z_0)^2}\right] - \displaystyle\sum_{j=1}^{4} U^{\mathrm{I}}_{3j}Y_{3j} \\
\dfrac{1}{b}u_{z2}(x,z,z_0) = -\dfrac{1}{4\pi(1-\nu_2)}\left[(1-2\nu_2)\ln\sqrt{\dfrac{x^2+(z-z_0)^2}{z_0^2}} - \dfrac{(z-z_0)^2}{x^2+(z-z_0)^2}\right] - \displaystyle\sum_{j=1}^{4} U^{\mathrm{I}}_{4j}Y_{4j}
\end{cases}, \tag{30}$$

where $Y_{ij}(x,z;z_0)$ are given in Appendix A and the matrix $\mathbf{U}^{\mathrm{I}}$ is given by (28). Stress components on which the continuity conditions were imposed are given by

$$\begin{cases}
\dfrac{1}{b}\sigma_{zz1}(x,z,z_0) = -\dfrac{\mu_1}{2\pi(1-\nu_1)}\dfrac{(z-z_0)[(z-z_0)^2-x^2]}{[x^2+(z-z_0)^2]^2} - \displaystyle\sum_{j=1}^{4} G^{\mathrm{I}}_{1j}I_{1j} \\
\dfrac{1}{b}\sigma_{zz2}(x,z,z_0) = -\dfrac{\mu_2}{2\pi(1-\nu_2)}\dfrac{(z-z_0)[(z-z_0)^2-x^2]}{[x^2+(z-z_0)^2]^2} - \displaystyle\sum_{j=1}^{4} G^{\mathrm{I}}_{2j}I_{2j} \\
\dfrac{1}{b}\sigma_{xz1}(x,z,z_0) = -\dfrac{\mu_1}{2\pi(1-\nu_1)}\dfrac{x[(z-z_0)^2-x^2]}{[x^2+(z-z_0)^2]^2} - \displaystyle\sum_{j=1}^{4} G^{\mathrm{I}}_{3j}I_{3j} \\
\dfrac{1}{b}\sigma_{xz2}(x,z,z_0) = -\dfrac{\mu_2}{2\pi(1-\nu_2)}\dfrac{x[(z-z_0)^2-x^2]}{[x^2+(z-z_0)^2]^2} - \displaystyle\sum_{j=1}^{4} G^{\mathrm{I}}_{4j}I_{4j}
\end{cases}, \tag{31}$$

where $I_{ij}(x,z;z_0)$ are given in Appendix A and G^{I} is given by (23). Other non-vanishing stress components are

$$\begin{cases}
\dfrac{1}{b}\sigma_{xx1}(x,z,z_0) = -\dfrac{\mu_1}{2\pi(1-\nu_1)}\dfrac{(z-z_0)[3x^2+(z-z_0)^2]}{[x^2+(z-z_0)^2]^2} + (2C_2-D)I_{11} - (C_2-D)I_{12} - 3(C_2-D)I_{13} + 2(C_2-D)I_{14} \\
\dfrac{1}{b}\sigma_{xx2}(x,z,z_0) = -\dfrac{\mu_2}{2\pi(1-\nu_2)}\dfrac{(z-z_0)[3x^2+(z-z_0)^2]}{[x^2+(z-z_0)^2]^2} - (2C_1+D)I_{21} - (C_1+D)I_{22} + (C_1-D)I_{23} \\
\dfrac{1}{b}\sigma_{yy1}(x,z,z_0) = -\dfrac{\mu_1\nu_1}{\pi(1-\nu_1)}\dfrac{(z-z_0)}{x^2+(z-z_0)^2} - 2\nu_1(C_2-D)(2I_{13}-I_{11}) \\
\dfrac{1}{b}\sigma_{yy2}(x,z,z_0) = -\dfrac{\mu_2\nu_2}{\pi(1-\nu_2)}\dfrac{(z-z_0)}{x^2+(z-z_0)^2} - 2\nu_2(C_1+D)I_{21}
\end{cases}, \tag{32}$$

where C_1, C_2, D are given by (24). By direct comparison it can be shown that the solutions above for σ_{xx1} in $x=0$ reproduce the results obtained by Cook (1971). If $\mu_2=0$, eqs (30)–(32) reproduce the solutions for an elementary dislocation problem in a half-space with a free surface (e.g. Bonafede & Danesi 1997).

Case II

If the dislocation surface extends from $z=z_0<0$ to $z=+\infty$ (i.e. if it cuts the interface $z=0$), the displacement field is given by

$$\begin{cases} \dfrac{1}{b}u_{x1}(x,z,z_0)=\dfrac{1}{2\pi}\left[-\operatorname{Arctan}\dfrac{z-z_0}{x}+\dfrac{1}{2(1-\nu_1)}\dfrac{x(z-z_0)}{x^2+(z-z_0)^2}\right]-\sum_{j=1}^{4}U^{II}_{2j}Y_{2j} \\ \dfrac{1}{b}u_{x2}(x,z,z_0)=\dfrac{1}{2\pi}\left[-\operatorname{Arctan}\dfrac{z-z_0}{x}+\dfrac{1}{2(1-\nu_2)}\dfrac{x(z-z_0)}{x^2+(z-z_0)^2}\right]-\sum_{j=1}^{4}U^{II}_{1j}Y_{1j} \\ \dfrac{1}{b}u_{z1}(x,z,z_0)=-\dfrac{1}{4\pi(1-\nu_1)}\left[(1-2\nu_1)\ln\sqrt{\dfrac{x^2+(z-z_0)^2}{z_0^2}}-\dfrac{(z-z_0)^2}{x^2+(z-z_0)^2}\right]-\sum_{j=1}^{4}U^{II}_{4j}Y_{4j} \\ \dfrac{1}{b}u_{z2}(x,z,z_0)=-\dfrac{1}{4\pi(1-\nu_2)}\left[(1-2\nu_2)\ln\sqrt{\dfrac{x^2+(z-z_0)^2}{z_0^2}}-\dfrac{(z-z_0)^2}{x^2+(z-z_0)^2}\right]-\sum_{j=1}^{4}U^{II}_{3j}Y_{3j} \end{cases}, \tag{33}$$

where

$$\mathbf{U}^{II}=\begin{pmatrix} -\dfrac{(1-\nu_2)}{\mu_2}C_1-\dfrac{(1-2\nu_2)}{2\mu_2}D & \dfrac{1}{2\mu_2}(C_1+D) & \dfrac{(3-4\nu_2)}{2\mu_2}(D+C_1) & -\dfrac{1}{\mu_2}(C_1+D) \\ \dfrac{(1-\nu_1)}{\mu_1}C_2-\dfrac{(1-2\nu_1)}{2\mu_1}D & \dfrac{1}{2\mu_1}(C_2-D) & -\dfrac{1}{2\mu_1}(D+C_2) & 0 \\ -\dfrac{(1-\nu_2)}{\mu_2}D-\dfrac{(1-2\nu_2)}{2\mu_2}C_1 & -\dfrac{1}{2\mu_2}(C_1+D) & \dfrac{(3-4\nu_2)}{2\mu_2}(D+C_1) & \dfrac{1}{\mu_2}(C_1+D) \\ \dfrac{(1-\nu_1)}{\mu_1}D-\dfrac{(1-2\nu_1)}{2\mu_1}C_2 & \dfrac{1}{2\mu_1}(C_2-D) & -\dfrac{1}{2\mu_1}(D+C_2) & 0 \end{pmatrix}. \tag{34}$$

From a comparison with the solutions for case I, we note that (33) and (34) can be obtained respectively from (30) and (28) by keeping the same expressions for the first part of the solution (the unbounded-medium solution, which accounts for the displacement discontinuity over the dislocation surface) and exchanging the roles of half-spaces 1 and 2 (i.e. $x\to -x$, $z\to -z$, $\mu_1\to\mu_2$ and $\nu_1\to\nu_2$) in the second part of the solution (the contribution of the strain function, which removes the discontinuities on the interface). Indeed, if such an exchange is performed, we must also change $C_1\to C_2$, $C_2\to C_1$, $D\to -D$ according to their definitions given in (24) these changes make the matrix $\mathbf{U}^{I}$ equal to $\mathbf{U}^{II}$ and $Y_{1j}(-z_0)=Y_{2j}(z_0)$, etc. It can be proved that these selection rules must hold, employing invariance arguments and the superposition principle.

Stress components on which the continuity conditions are to be imposed are given by

$$\begin{cases} \dfrac{1}{b}\sigma_{zz1}(x,z,z_0)=-\dfrac{\mu_1}{2\pi(1-\nu_1)}\dfrac{(z-z_0)[(z-z_0)^2-x^2]}{[x^2+(z-z_0)^2]^2}-\sum_{j=1}^{4}G^{II}_{2j}I_{2j} \\ \dfrac{1}{b}\sigma_{zz2}(x,z,z_0)=-\dfrac{\mu_2}{2\pi(1-\nu_2)}\dfrac{(z-z_0)[(z-z_0)^2-x^2]}{[x^2+(z-z_0)^2]^2}-\sum_{j=1}^{4}G^{II}_{1j}I_{1j} \\ \dfrac{1}{b}\sigma_{xz1}(x,z,z_0)=-\dfrac{\mu_1}{2\pi(1-\nu_1)}\dfrac{x[(z-z_0)^2-x^2]}{[x^2+(z-z_0)^2]^2}-\sum_{j=1}^{4}G^{II}_{4j}I_{4j} \\ \dfrac{1}{b}\sigma_{xz2}(x,z,z_0)=-\dfrac{\mu_2}{2\pi(1-\nu_2)}\dfrac{x[(z-z_0)^2-x^2]}{[x^2+(z-z_0)^2]^2}-\sum_{j=1}^{4}G^{II}_{3j}I_{3j} \end{cases}, \tag{35}$$

where

$$\mathbf{G}^{II}=\begin{pmatrix} -D & -(C_1+D) & C_1+D & 2(C_1+D) \\ -D & -(C_2-D) & C_2+D & 0 \\ C_1 & -(C_1+D) & -(C_1+D) & 2(C_1+D) \\ C_2 & C_2-D & -(C_2+D) & 0 \end{pmatrix}. \tag{36}$$

Other non-vanishing stress components are

$$\begin{cases} \dfrac{1}{b}\sigma_{xx1}(x,z,z_0) = -\dfrac{\mu_1}{2\pi(1-\nu_1)}\dfrac{(z-z_0)[3x^2+(z-z_0)^2]}{[x^2+(z-z_0)^2]^2} - (2C_2-D)I_{21} - (C_2-D)I_{22} + (C_2+D)I_{23} \\ \dfrac{1}{b}\sigma_{xx2}(x,z,z_0) = -\dfrac{\mu_2}{2\pi(1-\nu_2)}\dfrac{(z-z_0)[3x^2+(z-z_0)^2]}{[x^2+(z-z_0)^2]^2} + (2C_1+D)I_{11} - (C_1+D)I_{12} - 3(C_1+D)I_{13} + 2(C_1+D)I_{14} \\ \dfrac{1}{b}\sigma_{yy1}(x,z,z_0) = -\dfrac{\mu_1\nu_1}{\pi(1-\nu_1)}\dfrac{(z-z_0)}{x^2+(z-z_0)^2} - 2\nu_1(C_2-D)I_{21} \\ \dfrac{1}{b}\sigma_{yy2}(x,z,z_0) = -\dfrac{\mu_2\nu_2}{\pi(1-\nu_2)}\dfrac{(z-z_0)}{x^2+(z-z_0)^2} - 2\nu_2(C_1+D)(2I_{13}-I_{11}) \end{cases} \tag{37}$$

RESULTS AND CONCLUSIONS

A dislocation surface bounded in the dip direction and embedded in half-space 1 (Fig. 2, model A) can easily be obtained from the elementary dislocation solution for case I described above. Let $f(x, z; z_0)$ be any component of displacement, stress or strain generated by an elementary dislocation line in $x = 0$, $z = z_0$; exploiting the linearity of our equations, solutions for a dislocation open from $z = z_0$ to $z = z_0 + h$ are simply obtained as $f(x, z; z_0) - f(x, z; z_0 + h)$.

A dislocation surface bounded in the dip direction and cutting across the interface between half-spaces 1 and 2 (Fig. 2, model B) can be similarly obtained by subtracting the elementary dislocation solution for case I (dislocation line in $z_0 = h/2$) from the elementary solution for case II (dislocation line in $z_0 = -h/2$).

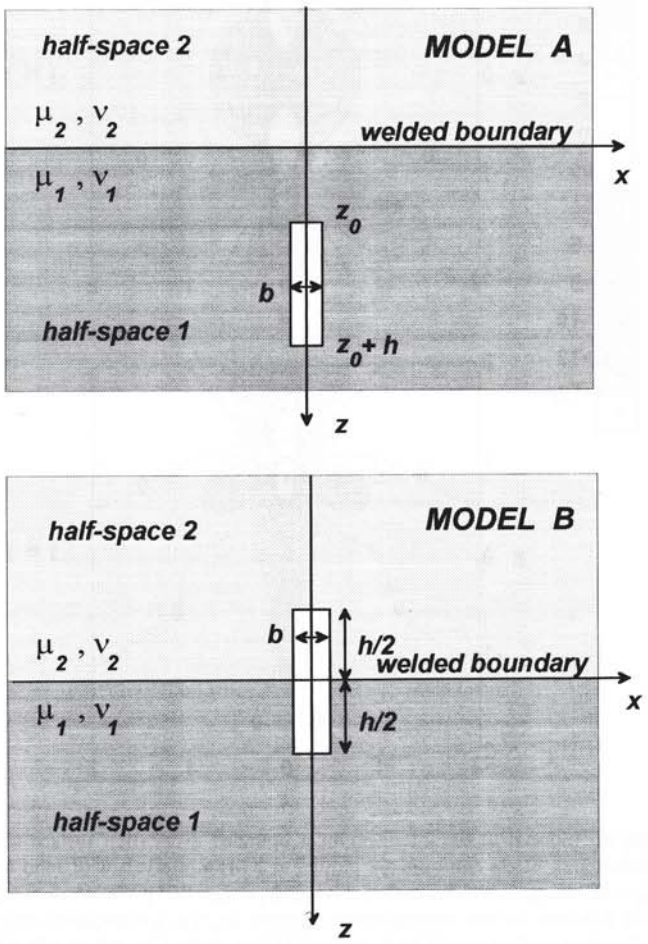

Figure 2. A closed Volterra dislocation can be obtained by superposing the elementary solution for a dislocation line in $z = z_0$ and Burgers vector b with the solution for a dislocation line in $z = z_0 + h$ and Burgers vector $-b$. In model A the dislocation surface is entirely embedded in half-space 1. In model B $z_0 = -h/2$ and the dislocation surface cuts symmetrically across the interface.

Stress components for both model A and model B are shown in Figs 3, 4, 5. Results are compared with solutions pertinent to a homogeneous medium with rigidity μ_1 and Poisson ratio ν_1 (obtained from eq. 2). In order to emphasize the role played by medium heterogeneities, we assumed $\mu_1 = 30$ GPa and $\mu_2 = 0.1\mu_1$, which are reasonable although extreme values for a transition

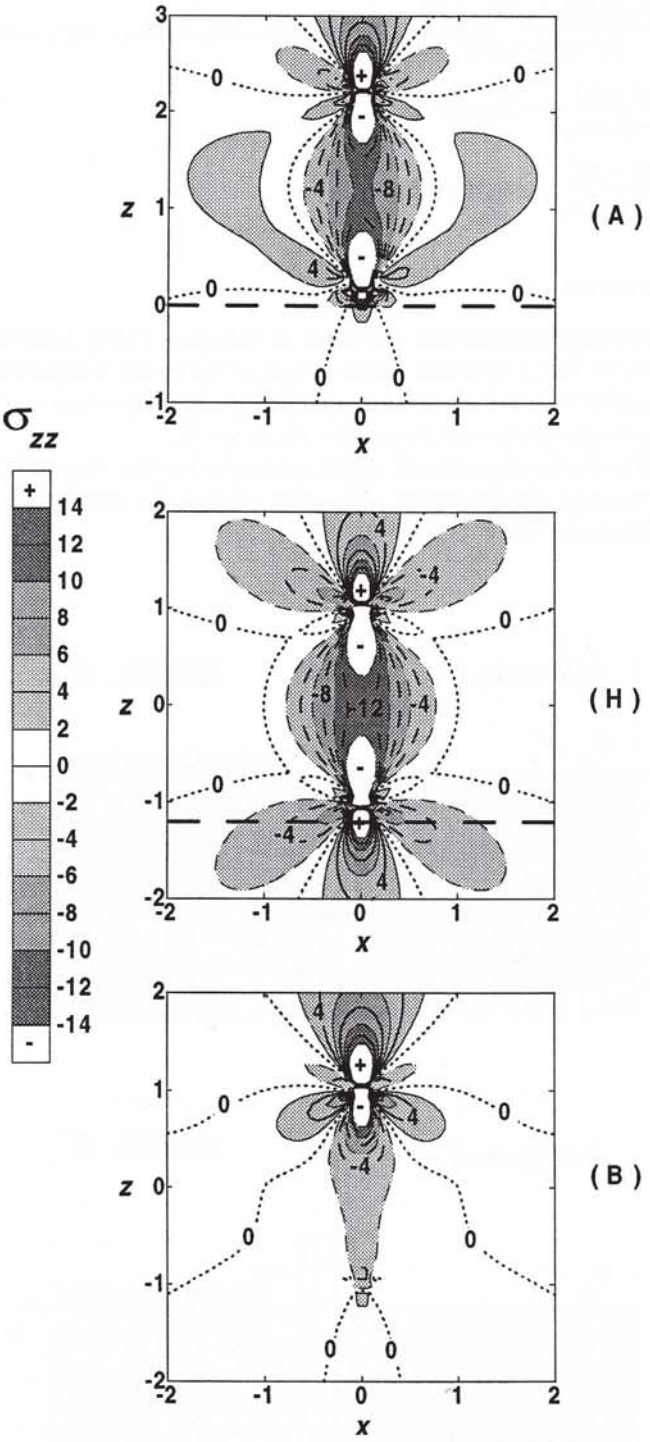

Figure 3. Map of the stress component σ_{zz} (normal to the interface) for a bounded dislocation surface with Burgers vector $b = 1$ m and length $h = 2$ km. Coordinates x and z are in kilometres. Stress contours are plotted at 2 MPa intervals with solid lines is positive (tensile), dashed lines is negative (compressive). (A) Model A: $z_0 = 200$ m, $\mu_1 = 30$ GPa and $\mu_2 = 0.1\ \mu_1$ ($\nu_1 = \nu_2 = 0.25$); the interface between half-spaces 1 and 2 is the plane $z = 0$, shown as a long-dashed line. (H) Solution for the homogeneous medium ($\mu_2 = \mu_1$), dislocation surface $-1 < z < +1$; the position of the interface of model A relative to the dislocation surface would be in $z = -1.2$ (long-dashed line) here. (B) Solution for model B: the interface is in $z = 0$ and should be compared with $z = 0$ in panel (H). Elastic constants as in (A), dislocation surface $-1 < z < +1$. Note that the domain shown for the coordinate z in (A) is different from that in (H) and (B). In each panel, + and − indicate regions within which σ_{xx} goes up to $+\infty$ or down to $-\infty$, respectively. Grey tones extend ± 2 MPa on both sides of contour lines labelled with multiples of 4 MPa.

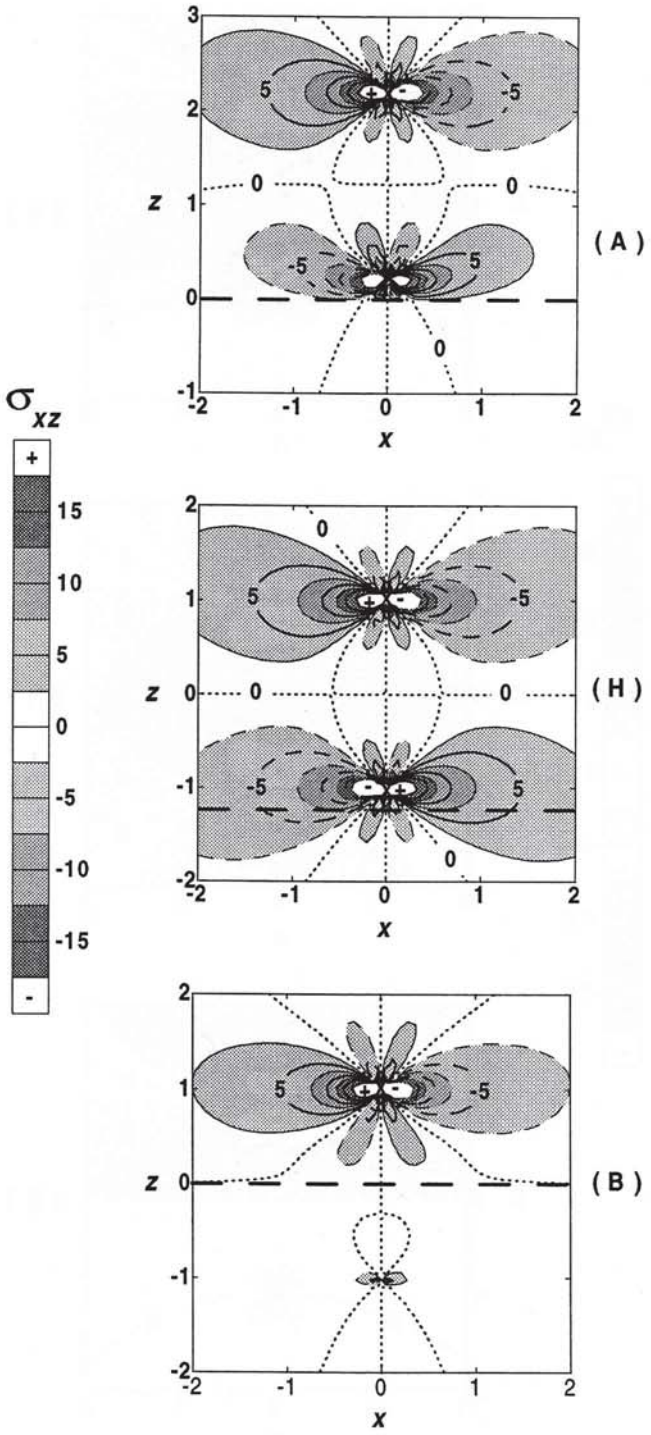

Figure 4. Map of the shear stress component σ_{xz}. (A) Layered medium in model A; (H) homogeneous medium; (B) layered medium in model B. Parameter values as for Fig. 3. Contour lines are drawn at 2.5 MPa intervals. Grey tones extend ± 2.5 MPa on both sides of contour lines labelled with multiples of 5 MPa.

from basaltic basement rock to volcano–sedimentary cover. We furthermore assume $z_0 = 200$ m and $h = 2$ km for model A, while in model B the dislocation cuts symmetrically across the interface (from $z = -h/2$ to $z = h/2$).

In Fig. 3 the normal stress σ_{zz} is plotted. This component is continuous across the interface, as it must be in order to comply with the welded-boundary conditions. The low rigidity of the half-space 2 ($z < 0$) makes the stress amplitude much lower there than in the homogeneous model, both in model A and in model B. Even in the harder half-space 1, stress values are generally lower than in the homogeneous model. In model A, this component of stress is small even in the high-rigidity region between the tip of the dislocation in $z = z_0$ and the interface $z = 0$; from a physical point of view, this behaviour can be ascribed to the fact that σ_{zz} is mostly dependent on $\partial u_z/\partial z$ and the displacement normal to the interface finds little opposition from the soft medium

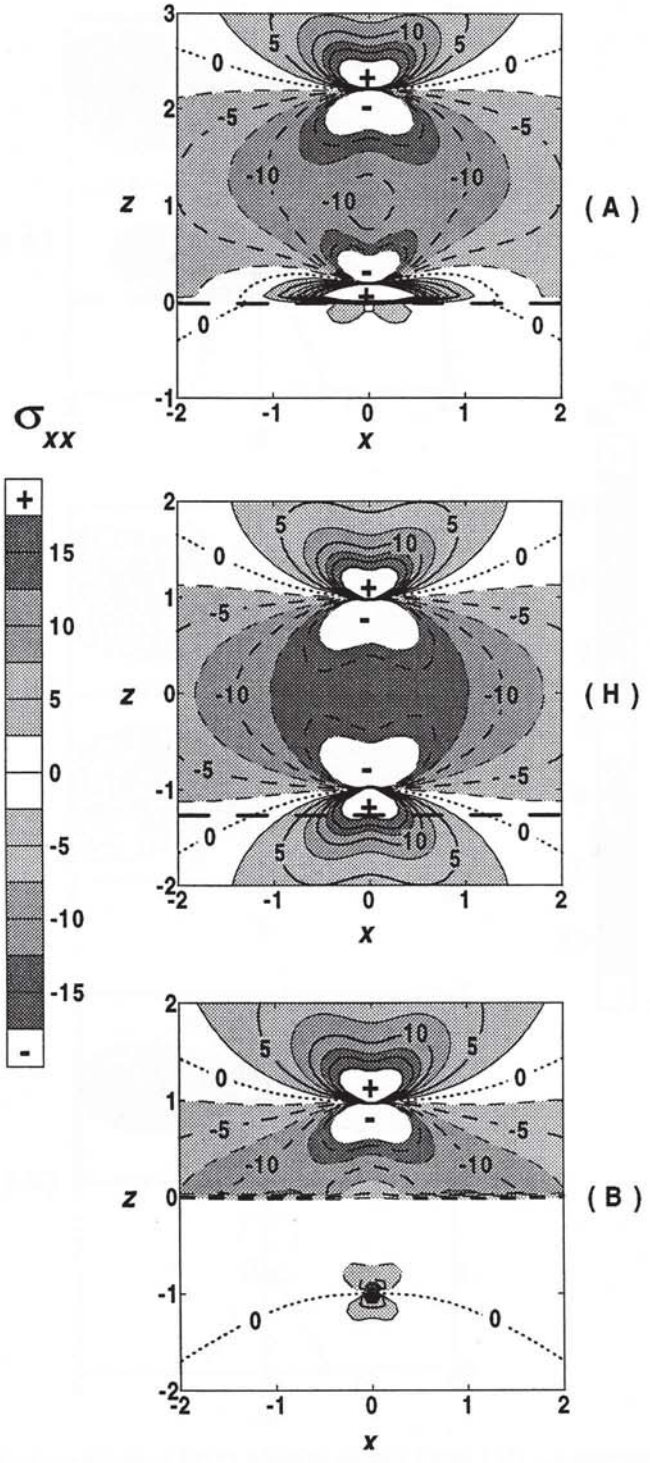

Figure 5. Map of the stress component σ_{xx} (normal to the dislocation plane). (A) Layered medium in model A; (H) homogeneous medium; (B) layered medium in model B. Parameter values as in Fig. 3. Note the wide stress concentration present below the interface in the layered model A. Contour lines are drawn at 2.5 MPa intervals. Grey tones extend ± 2.5 MPa on both sides of contour lines labelled with multiples of 5 MPa.

in $z < 0$. However, stress values higher than in the homogenous model can be found in model A, on both sides of the dislocation surface and at some distance from it.

In Fig. 4 the shear stress σ_{xz} is plotted. This component is also continuous across the interface. Compared with the homogeneous model, contour lines for the layered model A are deflected away from the interface and numerical values are generally lower, particularly near the interface. Considerations similar to the previous ones hold even in this case. Both the σ_{zz} and the σ_{xz} components seem to be significantly affected by the low rigidity of half-space 2 through the continuity condition.

In Fig. 5 the stress component σ_{xx} is shown; this component is discontinuous for the layered models A and B across the interface $z = 0$; when compared with the solution for a homogeneous medium (H), it appears that in model A a stronger and wider concentration of stress is present near the dislocation line $z = z_0$ on the hard side of the interface (the + region near $z = 0$). A qualitative reason for this result, which might seem to conflict with the behaviour of the other stress components, can be understood if we consider that the overall traction over any plane parallel to the dislocation plane $x = 0$ must be constant in order to attain equilibrium. Since the stress in the upper half-space is negligible, most of the traction exerted by the upper half-space in the homogeneous model must be supported by the thin layer $0 < z < z_0$ in the layered model A. The stress component σ_{xx} around the dislocation surface far away from the interface is also significantly affected by the presence of the interface: here, significantly lower stress amplitudes are present in the layered model A compared with the homogeneous model H. In model B a relative minimum is present for the stress amplitude near the dislocation–interface crossing, but further away from the centre of the dislocation surface, along the interface, stress values are higher than in model A or in model H.

It appears then that the welded-boundary conditions between the hard and soft half-spaces are responsible for major changes in all stress components. The continuous component σ_{xz} is generally smaller than in model H for both model A and model B, even in the harder half-space. The components σ_{zz} and σ_{xx} show a rather complex pattern of higher and lower values with respect to model H.

The previous method can easily be extended in principle to multilayered media or layered media with a free surface. The solution in the Fourier transform domain can be obtained easily by solving a linear system of dimension $4n$ (where n is the number of layer interfaces), similar to (17). On the other hand, the possibility of obtaining closed-form solutions is determined by our ability to invert the Fourier transforms analytically (which already seems to be unpracticable for $n = 2$).

However, even the simple two-layer model considered above offers the opportunity of studying the stress-field modifications induced by a tensile dislocation in the proximity of elastic heterogeneities. In particular, layering in the proximity of a tensile dislocation can be responsible for significant changes in the stress field near the interface, which would be nearly impossible to predict intuitively. Such changes need to be taken into account when interpreting seismicity induced by dyke injection episodes along rift zones and in volcanic regions. In this respect, the role of structural discontinuities in concentrating stress changes is very similar to that analysed for strike-slip earthquakes by Rybicki (1971, 1973). Employing an anti-plane dislocation model (source model with constant Burgers vector in the y-direction), he reached the conclusion that stresses generated by strike-slip earthquakes 'acting on inhomogeneities of the medium, result in aftershock generation'. As in the present paper, (in which σ_{xx} is the stress component which suffers the greatest changes due to layering), the major factor responsible for stress concentration in anti-plane dislocation models was the discontinuous stress component (σ_{yx}, employing the present choice of coordinates).

Returning to tensile dislocations, it is noted that σ_{xx} drops abruptly while going from layer 2 to layer 1, so that dyke propagation across a structural discontinuity might be inhibited even in the presence of positive bouyancy. However, a physically sounder model of dyke emplacement and propagation is a 'crack model' in which the overpressure within the magma filling the dyke is assigned, instead of constant opening (the Burgers vector). Solutions in the present paper yield the integral kernels required to set up a crack model. The crack problem, however, involves several additional problems which require lengthy treatment. These will be considered in another paper.

ACKNOWLEDGMENTS

Useful comments and suggestions by T. Dahm and K. R. Rybicki on an earlier version of the manuscript are gratefully acknowledged. Work was performed with financial contributions from C.N.R. Gruppo Nazionale per la Vulcanologia and from the European Commission under contract ENV4-CT96-0252.

REFERENCES

Bonaccorso, A. & Davis, P.M., 1993. Dislocation modelling of the 1989 dyke intrusion into the flank of Mount Etna, Sicily, *J. geophys. Res.*, **98,** 4261–4268.

Bonafede, M. & Danesi, S., 1997. Near-field modifications of stress induced by dyke injection at shallow depth, *Geophys. J. Int.*, **130,** 433–448.

Cayol, V., 1996. Analyse élastostatique tridimensionelle du champ de déformations des édifices volcaniques par éléments frontières mixtes, *Thèse de doctorat,* Université de Paris VII.

Cocina, O., Neri, G., Privitera, E. & Spampinato, S., 1996a. Earthquake and stress tensor space-time distribution at Mount Etna before the 1991–1993 volcanic eruption, *Acta Vulcanol.*, **8,** 15–22.

Cocina, O., Neri, G., Privitera, E. & Spampinato, S., 1996b. Stress tensor computations in the Mount Etna area (southern Italy) and tectonic implications, *J. Geodyn.*, **23,** 109–127.

Cook, T.S., 1971. Flaws in wedges, *PhD thesis,* Lehigh University.

Crouch, S.L. & Starfield, A.M., 1990. *Boundary Element Methods in Solid Mechanics,* Unwin Hyman, London.

Dahm, T., 1996. Elastostatic simulation of dislocation sources in heterogeneous stress fields and multilayered media having irregular interfaces, *Phys. Chem. Earth,* **21,** 241–245.

Dahm, T. & Brandsdottir, B., 1997. Moment tensors of micro-earthquakes from the Eyjafjallajökull volcano in south Iceland, *Geophys. J. Int.*, **130,** 183–192.

Davis, P.M., 1983. Surface deformation associated with a dipping hydrofracture, *J. geophys. Res.*, **88,** 5826–5834.

Dieterich, J.H. & Decker, R.H., 1975. Finite element modeling of surface deformation associated with volcanism, *J. geophys. Res.*, **80,** 4094.

Erdogan, F., Gupta, G.D. & Cook, T.S., 1973. Numerical solution of singular integral equations, in *Mechanics of Fracture,* Vol. I, pp. 368–425, ed. Sih, G.C., Noordhoff, the Netherlands.

Fernandez, J. & Rundle, J.B., 1994. Gravity changes and deformation due to a magmatic intrusion in a two-layered crustal model, *J. geophys. Res.*, **99,** 2737–2746.

Ferrucci, F. & Patanè, D., 1993. Seismic activity accompanying the outbreak of the 1991-93 eruption of Mt. Etna, *J. Volc. Geotherm. Res.*, **57,** 125–135.

Fung, Y.C., 1965. *Foundations of Solid Mechanics,* Prentice Hall, Englewood Cliffs, NJ.

Landau, L.D. & Lifschitz, E., 1967. *Théorie de l'élasticité,* Éditions Mir, Moscou.

Lénat, J.F., Batchélery, P., Bonneville, A., Tarits, P., Cheminée, J.L. & Delorme, H., 1989a. The December 4, 1983 to February 18, 1984 eruption of Piton de la Fournaise (la Réunion, Indian Ocean): description and interpretation, *J. Volc. Geotherm. Res.*, **36,** 87–112.

Lénat, J.F., Batchèlery, P., Bonneville, A. & Hirn, A., 1989b. The beginning of the 1985-87 eruptive cycle at Piton de la Fournaise (La Reunion); new insights in the magmatic and volcano-tectonic systems, *J. Volc. Geotherm. Res.*, **36,** 209–232.

Lister, J.R., 1991. Steady solutions for feeder dykes in density-stratified lithosphere, *Earth plant. Sci. Lett.*, **107,** 233–242.

Maruyama, T., 1964. Statical elastic dislocations in an infinite and semi-infinite medium, *Bull. Earthq. Res. Inst. Tokyo Univ.*, **42,** 289–368.

Murray, J.B., 1994. Elastic model of the actively intruded dyke feeding the 1991-93 eruption of Mt. Etna derived from ground deformation measurements, *Acta Vulcanol.*, **4,** 97–99.

Okada, Y., 1992. Internal deformation due to shear and tensile faults in a half-space, *Bull. seism. Soc. Am.*, **82,** 1018–1040.

Pollard, D.D. & Holzhausen, G., 1979. On the mechanical interaction between a fluid-filled fracture and the earth's surface, *Tectonophysics,* **53,** 27–57.

Pollard, D.D., Delaney, P.T., Duffield, W.A., Endo, E.T. & Okamura, A.T., 1983. Surface deformation in volcanic rift zones, *Tectonophysics,* **94,** 541–584.

Roth, F., 1990. Subsurface deformations in a layered half-space, *Geophys. J. Int.*, **103,** 147–155.

Rundle, J.B., 1980. Static elastic-gravitational deformation of a layered half-space by point couple sources, *J. geophys. Res.*, **85,** 5355–5363.

Rybicki, K.R., 1971. The elastic residual field of a very long strike-slip fault in the presence of a discontinuity, *Bull. seism. Soc. Am.*, **61,** 79–92.

Rybicki, K.R., 1973. Analysis of aftershocks on the basis of dislocation theory, *Phys. Earth planet. Inter.*, **7,** 409–422.

Zlotnicki, J., Ruegg, J.C., Bachelery, P. & Blum, P.A., 1990. Eruptive mechanism on Piton de la Founaise volcano associated with the December 4, 1983 and January 18, 1984 eruptions from ground deformation monitoring and photogrammetric surveys, *J. Volc. Geotherm. Res.*, **40,** 197–217.

APPENDIX A: ANALYTIC EXPRESSIONS FOR I_{ij} AND Y_{ij} FUNCTIONS

The integrals $I_{ij}(x, z; z_0)$ appearing in (22) and (25) are defined and computed below:

$$\begin{cases} I_{11}=\displaystyle\int_0^{+\infty} \mathrm{e}^{-k(z+z_0)}\cos kx\,dk=\frac{z_0+z}{[x^2+(z+z_0)^2]} \\ I_{21}=\displaystyle\int_0^{+\infty} \mathrm{e}^{-k(-z+z_0)}\cos kx\,dk=\frac{z_0-z}{[x^2+(z-z_0)^2]} \\ I_{31}=\displaystyle\int_0^{+\infty} \mathrm{e}^{-k(z+z_0)}\sin kx\,dk=\frac{x}{[x^2+(z+z_0)^2]} \\ I_{41}=\displaystyle\int_0^{+\infty} \mathrm{e}^{-k(-z+z_0)}\sin kx\,dk=\frac{x}{[x^2+(z-z_0)^2]} \end{cases}, \quad \begin{cases} I_{12}=z\displaystyle\int_0^{+\infty} k\,\mathrm{e}^{-k(z+z_0)}\cos kx\,dk=z\frac{(z+z_0)^2-x^2}{[x^2+(z+z_0)^2]^2} \\ I_{22}=z\displaystyle\int_0^{+\infty} k\,\mathrm{e}^{-k(-z+z_0)}\cos kx\,dk=z\frac{(z-z_0)^2-x^2}{[x^2+(z-z_0)^2]^2} \\ I_{32}=z\displaystyle\int_0^{+\infty} k\,\mathrm{e}^{-k(z+z_0)}\sin kx\,dk=\frac{2xz(z_0+z)}{[x^2+(z+z_0)^2]^2} \\ I_{42}=z\displaystyle\int_0^{+\infty} k\,\mathrm{e}^{-k(-z+z_0)}\sin kx\,dk=\frac{2xz(z_0-z)}{[x^2+(z-z_0)^2]^2} \end{cases},$$

$$\begin{cases} I_{13}=z_0\displaystyle\int_0^{+\infty} k\,\mathrm{e}^{-k(z+z_0)}\cos kx\,dk=z_0\frac{(z+z_0)^2-x^2}{[x^2+(z+z_0)^2]^2} \\ I_{23}=z_0\displaystyle\int_0^{+\infty} k\,\mathrm{e}^{-k(-z+z_0)}\cos kx\,dk=z_0\frac{(z-z_0)^2-x^2}{[x^2+(z-z_0)^2]^2} \\ I_{33}=z_0\displaystyle\int_0^{+\infty} k\,\mathrm{e}^{-k(z+z_0)}\sin kx\,dk=\frac{2xz_0(z_0+z)}{[x^2+(z+z_0)^2]^2} \\ I_{43}=z_0\displaystyle\int_0^{+\infty} k\,\mathrm{e}^{-k(-z+z_0)}\sin kx\,dk=\frac{2xz_0(z_0-z)}{[x^2+(z-z_0)^2]^2} \end{cases}, \quad \begin{cases} I_{14}=zz_0\displaystyle\int_0^{+\infty} k^2\,\mathrm{e}^{-k(z+z_0)}\cos kx\,dk=2zz_0\frac{(z_0+z)[(z+z_0)^2-3x^2]}{[x^2+(z+z_0)^2]^3} \\ I_{24}=zz_0\displaystyle\int_0^{+\infty} k^2\,\mathrm{e}^{-k(-z+z_0)}\cos kx\,dk=2zz_0\frac{(z_0-z)[(z-z_0)^2-3x^2]}{[x^2+(z-z_0)^2]^3} \\ I_{34}=zz_0\displaystyle\int_0^{+\infty} k^2\,\mathrm{e}^{-k(z+z_0)}\sin kx\,dk=2zz_0\frac{x[3(z_0+z)^2-x^2]}{[x^2+(z+z_0)^2]^3} \\ I_{44}=zz_0\displaystyle\int_0^{+\infty} k^2\,\mathrm{e}^{-k(-z+z_0)}\sin kx\,dk=2zz_0\frac{x[3(z_0-z)^2-x^2]}{[x^2+(z-z_0)^2]^3} \end{cases}.$$

The functions $Y_{ij}(x, z; z_0)$ appearing in (27) are given below: (A1)

$$\begin{cases} Y_{11}=\mathrm{Arctan}\dfrac{z_0+z}{x} \\ Y_{21}=\mathrm{Arctan}\dfrac{z_0-z}{x} \\ Y_{31}=\ln\sqrt{\dfrac{x^2+(z+z_0)^2}{z_0^2}} \\ Y_{41}=\ln\sqrt{\dfrac{x^2+(z-z_0)^2}{z_0^2}} \end{cases}, \quad \begin{cases} Y_{12}=\dfrac{zx}{x^2+(z+z_0)^2} \\ Y_{22}=\dfrac{zx}{x^2+(z-z_0)^2} \\ Y_{32}=-\dfrac{z(z_0+z)}{x^2+(z+z_0)^2} \\ Y_{42}=-\dfrac{z(z_0-z)}{x^2+(z-z_0)^2} \end{cases}, \quad \begin{cases} Y_{13}=\dfrac{z_0x}{x^2+(z+z_0)^2} \\ Y_{23}=\dfrac{z_0x}{x^2+(z-z_0)^2} \\ Y_{33}=-\dfrac{z_0(z_0+z)}{x^2+(z+z_0)^2} \\ Y_{43}=-\dfrac{z_0(z_0-z)}{x^2+(z-z_0)^2} \end{cases}, \quad \begin{cases} Y_{14}=\dfrac{2zz_0x(z_0+z)}{[x^2+(z+z_0)^2]^2} \\ Y_{24}=\dfrac{2zz_0x(z_0-z)}{[x^2+(z-z_0)^2]^2} \\ Y_{34}=\dfrac{zz_0[x^2-(z_0+z)^2]}{[x^2+(z+z_0)^2]^2} \\ Y_{44}=\dfrac{zz_0[x^2-(z_0-z)^2]}{[x^2+(z-z_0)^2]^2} \end{cases}. \quad \text{(A2)}$$